Korean J. Chem. Eng., 33(10), 2982-2989 (2016)
DOI: 10.1007/s11814-016-0140-4

pISSN: 0256-1115
eISSN: 1975-7220

The selectivity of imidazolium-based ionic liquids with different anions to BTX aromatics in hexane at 298.15 K and atmospheric pressure

Kyeong-Ho Lee, Soo-Hyun You, and So-Jin Park†

Department of Chemical Engineering, Chungnam National University, 220 Gung-dong, Yuseong-gu, Daejeon 34134, Korea
(*Received 20 March 2016 • accepted 14 May 2016*)

Abstract−The selectivity of alkyl-substituted imidazolium cation-based ionic liquids (ILs) with different anion: Tf_2N, PF_6, Tf_2N and BF_4, namely 1-Butyl-3-methylimidazolium bis(trifluoromethyl sulfonyl)imide ([BMIM][Tf_2N]), 1-Butyl-3-methylimidazolium hexafluorophosphate ([BMIM][PF_6]), 1-Ethyl-3-methylimidazolium bis(trifluoromethylsulfonyl)imide ([EMIM][Tf_2N]), 1-Methyl-3-octyl imidazolium tetrafluoroborate ([OMIM][BF_4]), was tested for the extraction of benzene, toluene and p-xylene(BTX) aromatics with hexane mixtures. Liquid-liquid equilibrium (LLE) data were determined for the six ternary mixtures {hexane (1)+BTX (2)+ILs (3)} at 298.15 K and atmospheric pressure. In addition, binary LLE data from 293.15 K to 318.15 K are also reported for the system {hexane (1)+[BMIM][Tf_2N] (2)}. The ternary experimental LLE data were satisfactorily correlated with the NRTL activity coefficient model. The degree of consistency of the tie lines was estimated by using the Othmer-Tobias equation, for which a good linear correlation coefficient (R^2) was obtained. As a result, the selectivity of ILs as potential solvents for the extraction of BTX from aliphatic components was found to be much higher than unity and PF_6 anion showed higher selectivity compared to other anions.

Keywords: Liquid-liquid Equilibrium, Separation, Aliphatic, Aromatic, Ionic Liquid

INTRODUCTION

Aromatic compounds are obtained almost exclusively from reformed naphtha. These aromatic components are usually separated from the aliphatic hydrocarbons through liquid extraction, since the boiling points of these hydrocarbons occur in a close range and several of these liquid combinations form azeotropes [1,2].

A large number of ionic liquids (ILs) have unique properties, such as a low vapor pressure at ambient pressure, excellent thermal and chemical stability, and favorable solvating properties [3,4]. Therefore, ILs have been considered promising solvents to replace traditional organic solvents in liquid extraction processes. ILs have attracted the attention of numerous researchers interested in using them for the liquid extraction of aromatics from aliphatic hydrocarbons instead of using environmentally unfriendly organic solvents [5-8]. Moreover, the regeneration costs of ILs are lower than those of organic solvents such as sulfolane, which has a boiling point of 287.3 °C [9]. The imidazolium based ILs have been widely used as solvents and applied to the many industrial processes, including in the extraction of aromatic hydrocarbons of this research. Therefore, we want to select suitable anion of ionic liquids for the separation of aromatic hydrocarbons from aliphatic hydrocarbons by means of comparing experimental selectivity between anions and also comparing with those found in the literature. We investigated the following imidazolium-based ionic liquids with different anions: [BMIM][Tf_2N], [BMIM][PF_6], [EMIM][Tf_2N], and [OMIM][BF_4].

To test the selectivity of the ionic liquids as solvents in extraction processes, knowledge of the liquid-liquid equilibrium (LLE) data between related immiscible phases is essential. Therefore, we have measured the LLE data first for the following hexane+benzene mixtures containing ILs as solvent: {hexane (1)+benzene (2)+[BMIM][Tf_2N] (3)}, {hexane (1)+benzene (2)+[BMIM][PF_6] (3)}, {hexane (1)+benzene (2)+[EMIM][Tf_2N] (3)}, {hexane (1)+benzene (2)+[OMIM][BF_4] (3)} at 298.15 K and atmospheric pressure. And then, we measured LLE data for {hexane (1)+toluene (2)+[BMIM][PF_6] (3)} and {hexane (1)+p-xylene (2)+[BMIM][PF_6] (3)} systems under the same conditions, since [BMIM][PF_6] had better selectivity than other ILs in aforementioned benzene contained systems. For the case of [BMIM][Tf_2N], [BMIM][PF_6] and [EMIM][Tf_2N], the experimental LLE data with hexane and benzene are available in the literature [10-12]. However, these data ignored the solubility of ILs in hexane rich phase because dissolved mass of ILs was insignificant. Actually, the solubility of [BMIM][Tf_2N] in hexane phase from directly determined binary LLE data in this work was ca. 0.3% at 298.15 K. We reported, therefore, ternary LLE data with considering of ILs' solubility in hexane phase for [BMIM][Tf_2N], [BMIM][PF_6] and [EMIM][Tf_2N], and in addition, the new data as far as we know, for [OMIM][BF_4] and also for toluene and p-xylene mixtures with [BMIM][PF_6]. The binary LLE for {hexane (1)+[BMIM][Tf_2N] (2) from 293.15 K to 318.15 K was also reported. The determined equilibrium liquid phase compositions were correlated by using the nonrandom two-liquid (NRTL) thermodynamic model for all the systems. The reliability of the experimental tie-line data was ascertained by using the Othmer-Tobias correlating equations [13,14]. And then, the suitability of these ILs as solvents was ana-

†To whom correspondence should be addressed.
E-mail: sjpark@cnu.ac.kr

lyzed by calculating the selectivity (*S*) from the experimental LLE data. These *S* values of benzene contained systems were compared with those of organic solvents: acetonitrile and sulfolane.

EXPERIMENTAL SECTION

1. Materials

Hexane (C_6H_{14}, M=86.18 g·mol^{-1}, >95.0%, CAS-RN 110-54-3), benzene (C_6H_6, M=78.11 g·mol^{-1}, >99.5%, CAS-RN 7143-2), p-xylene (C_8H_{10}, M=106.17 g·mol^{-1}, >98.5%, CAS-RN 106-42-3) were supplied by Junsei Chemical. [BMIM][Tf_2N] ($C_{10}H_{15}F_6N_3O_4S_2$, M=419.36 g·mol^{-1}, CAS-RN 174899-83-3), [BMIM][PF_6] ($C_8H_{15}F_6N_2P$, M=284.18 g·mol^{-1}, >97%, CAS-RN 174501-64-5), [EMIM][Tf_2N] ($C_8H_{11}F_6N_3O_4S_2$, M=391.31 g·mol^{-1}, >98%, CAS-RN 174899-82-2), [OMIM][BF_4] ($C_{12}H_{23}BF_4N_2$, M=282.13 g·mol^{-1}, >97%, CAS-RN 244193-52-0) were supplied by the Sigma-Aldrich. Toluene (C_7H_8, M=92.14 g·mol^{-1}, >99.0% CAS-RN 108-88-3) was supplied by Wako. All chemicals were used after water drying using molecular sieves with a pore diameter of 0.3 nm. The purity of the chemicals was determined by gas chromatography (GC) and by comparing the density with the values reported in the literature. In addition, the water content of the chemicals was determined by using Karl-Fischer titration (Metrohm 684 KF-Coulometer). The water content of the hexane, benzene, toluene and p-xylene was less than 3.5 ppm, whereas that of the ILs was less than 18.3 ppm. The experimental physical properties (purity, density, and refractive index) of the pure components are reported and compared with the literature data [15-23] in Table 1. The small differences between the experimental and literature data may be mainly attributed to the presence of water and non-volatile impurities in the samples.

2. Apparatus and Procedure

2-1. Densities and Refractive Indices of Pure Components

Before every LLE measurement, the densities and refractive indices of the chemicals were measured by a digital vibrating glass tube densimeter (Anton Paar, model DMA 5000) and digital precision refractometer (model RA-520N, KEM) to test the purity of the samples. The manufacturer's stated accuracy of the densitometer was ±5×10^{-6} g·cm^{-3}, while the refractometer was 5×10^{-5} within a range of 1.32 to 1.40 and 1×10^{-4} within a range of 1.40 to 1.58. The standard deviation of the measurement for the density and refractive index, S(X) was calculated from the equation below:

$$S(X)=\sqrt{\frac{\Sigma_i^N(X_i-\overline{X})^2}{(N-1)}} \quad (1)$$

where X_i is the experimental property data of the component I, $\overline{X}$ is the mean of multiple experimental data points, and N is the number of experimental data points. The standard deviation calculated in this work has roughly 68% of probability. That is, 0.68 level of confidence. And the standard uncertainty was quite referring to the degree of repeatability.

By the way, for the density measurement, Laesecke et al. [24] and Fortin et al. [25] reported more realistic averaged combined standard uncertainty ($u_c(\rho)$) for N density measurements. It can be expressed like as:

$$u_c(\rho)=\sqrt{\frac{1}{N}S_\rho^2+u_\gamma^2+u_i^2+u_T^2} \quad (2)$$

where S_ρ, u_γ, u_i, u_T are uncertainty due to the standard deviation of the average, resolution of the instrument, instrument's varied response with density range, and the contribution due to the uncertainty in measured temperature, respectively. In this work, S_ρ=3.7×10^{-5} g·cm^{-3}, u_γ=1×10^{-5} g·cm^{-3}, u_i=3.3×10^{-5} g·cm^{-3} and u_T=1×10^{-5} g·cm^{-3}. Therefore, the averaged combined standard uncertainty was calculated as $u_c(\rho)$=4×10^{-5} g·cm^{-3} from Eq. (2).

However, in the case of ionic liquids, the impurity of sample makes the standard uncertainty much larger according to Chirico et al. [26]. Therefore, when we take account of impurity of ionic liquids in this work, the standard uncertainty is larger since the impurity of ionic liquids can in no way be negligible in this work.

The combined standard uncertainty of the refractive indices ($u(n_D)$) was calculated according to Eq. (3).

$$u_c(n_D)=\sqrt{\frac{1}{N}S_{nD}^2+u_\gamma^2+u_i^2} \quad (3)$$

The numerical values of each term were S_{nD}=3.5×10^{-4}, u_γ=2×10^{-5} and u_i=2.7×10^{-4} in this work. Therefore, the combined standard uncertainty of the refractive indices was estimated as $u_c(n_D)$=3×10^{-4}.

2-2. Liquid-liquid Equilibrium

The LLE measurement involved measuring the end point of tie-

Table 1. GC analysis, density (ρ) and refractive index (n_D) of pure components at T=298.15 K

Chemical	GC analysis (wt%)	ρ/g·cm^{-3} [a]		n_D [b]	
		Exp. value	Lit. value	Exp. value	Lit. value
Hexane	>99.8	0.65721	0.65512 [15]	1.3742	1.3725 [15]
Benzene	>99.6	0.87373	0.8738 [16]	1.4975	1.4978 [17]
Toluene	>99.6	0.86234	0.86233 [18]	1.4936	1.49413 [19]
p-Xylene	>99.7	0.85678	0.85670 [20]	1.4928	1.49286 [21]
[BMIM][Tf_2N]	-	1.43624	1.436 [22]	1.4269	-
[BMIM][PF_6]	-	1.34393	1.368 [22]	1.4090	-
[EMIM][Tf_2N]	-	1.51650	1.519 [22]	1.4226	-
[OMIM][BF_4]	-	1.03555	1.0530 [23]	1.4328	-

[a]Combined standard uncertainty u_c is $u_c(\rho)$=4×10^{-5} g·cm^{-3} and standard uncertainty u is u(T)=0.01 K

[b]Combined standard uncertainty u_c is $u_c(n_D)$=3×10^{-4} and standard uncertainty u is u(T)=0.05 K

lines for all the binary and ternary systems. The system that was used for the analytical LLE determination consists of an equilibrium double-glassed vessel (custom-designed and built), a thermostat (Lauda MD 20 with DLK15 cooler), temperature measurement equipment (AΣA F250), and magnetic stirrer (Corning PC-320). The uncertainty of temperature inside the equilibrium cell was 0.02 K. The sample mixtures were prepared by adding aromatics (BTX) to the mother solution consisting of a mixture of hexane and the IL. After that, the sample mixture was stirred in the equilibrium vessel for about 6 h and allowed to settle for more than 12 h at constant system temperature. Samples of the upper and lower phases were cautiously taken with a long-needled syringe to avoid the contamination of each phase. The equilibrium mass fraction was analyzed by dividing each sample into two portions, 0.1 mL and 1 mL, of which the former was used for GC analysis and the latter for the quantitative analysis of the ILs to determine the mass difference after drying in a vacuum oven. Drying was continued until the organic matter, hexane and benzene, had completely evaporated, i.e., after 24 h at 353.15 K. The precision of quantitative analysis by this drying method was estimated better than $\pm 3\times10^{-4}$. The weight of samples was determined using a microbalance (OHAUS Co. DV215CD) with a precision of 1×10^{-5} g. And for analysis of organic sample, an HP 6890N GC equipped with a thermal conductivity detector (TCD) and capillary column: HP-FFAP (polyethylene glycol TPA, 25 m×0.20 mm×0.30 μm) was used. High purity helium gas was used as carrier gas. The injector and detector temperatures were set to 503.15 K and 523.15 K, respectively. The oven temperature was retained at 333.15 K for 4 min and was then increased at a rate of 50 °C/min to reach a final temperature of 503.15 K, which was maintained for 8 min [27]. For the calculation of the accurate mass fractions of the organics by GC, the response factor of hexane and benzene was determined by using self-made standards. This procedure has been described in detail elsewhere [28]. The equilibrium composition of LLE was calculated as mass fraction. The uncertainty of weight fraction determination by GC was estimated less than 1×10^{-4} according to Eq. (1), and the precision (repeatability) of aforementioned quantitative analysis of ionic liquid by drying method was 3×10^{-4}. Therefore, the combined standard uncertainty of LLE measurement, $u_c(W)$ was estimated less than 3×10^{-4} from Eq. (4).

$$u_c(W)=\sqrt{u_G^2+u_D^2} \quad (4)$$

where u_G is uncertainty of GC analysis and u_D is the uncertainty of quantitative analysis of ionic liquid by drying method.

RESULTS AND DISCUSSION

1. Binary Mixtures with Hexane+Ionic Liquids

The determined LLE for the binary system for {hexane (1)+[BMIM][Tf_2N] (2)} at 293.15, 298.15, 303.15, 308.15, 313.15 and 318.15 K are listed in Table 2 and plotted in Fig. 1. As illustrated, only small amounts of hexane and ionic liquid were dissolved in the opposite phase. Hexane was dissolved more in [BMIM][Tf_2N] than [BMIM][Tf_2N] in hexane. The common NRTL activity coefficient model was applied to correlate the experimental binary LLE data, and the results are listed in Table 3. The NRTL model correlated the experimental data well within the mean deviation ($|\Delta w_1|_{av.}=\Sigma_{k=1}^{NDP}|w_{1,exp}-w_{1,cal}|_k/NDP$) of 2×10^{-4}. Where NDP is the number of data points.

Table 2. Experimental LLE data for the binary system of {hexane (1)+[BMIM][Tf_2N] (2)}

T/K	w_1	
	w_1^h	w_1^i
293.15	0.9889	0.0039
298.15	0.9884	0.0041
303.15	0.9875	0.0041
308.15	0.9865	0.0041
313.15	0.9841	0.0042
318.15	0.9780	0.0043

Combined standard uncertainty u_c is $u_c(w)=3\times10^{-4}$ and standard uncertainty u is u(T)=0.02 K

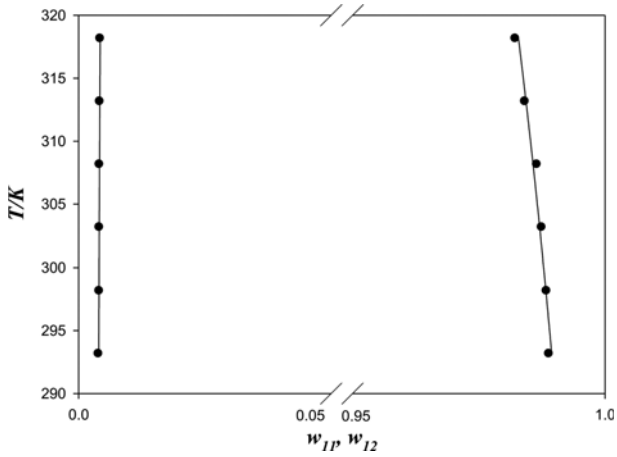

Fig. 1. LLF for the binary system; ●, {hexane (1)+[BMIM][Tf_2N] (2)}; solid curves were calculated from NRTL equation.

Table 3. The G^E model parameters and mean deviation between the calculated and experimental for the binary system

System	NRTL parameters (α_{ij}=0.20)			$\|\Delta w_1\|_{av.}$
	i-j	a_{ij} (K)	b_{ij}	
{Hexane (1)	1-2	1699.39	−1.07	0.0002
+[BMIM][Tf_2N] (2)}	2-1	150.27	1.77	

Parameters (K): $\Delta g_{ij}/R=a_{ij}+b_{ij}T$

2. Ternary Mixtures with Hexane+BTX Aromatics+Ionic Liquids

The LLE compositions that were determined for the ternary systems:{hexane (1)+benzene (2)+[BMIM][Tf_2N] (3)}, {hexane (1)+benzene (2)+[BMIM][PF_6] (3)}, {hexane (1)+benzene (2)+[EMIM][Tf_2N] (3)}, {hexane (1)+benzene (2)+[OMIM][BF_4] (3)}, {hexane (1)+toluene (2)+[BMIM][PF_6] (3)}, {hexane (1)+p-xylene (2)+[BMIM][PF_6] (3)} at 298.15 K and atmospheric pressure are given in Table 4 with the calculated distribution ratio (D) and selectivity (S) data. The experimental and calculated equilibrium compositions and tie-lines of each system were also plotted in the form of

Gibbs triangles in Figs. 2-7. The calculated values were obtained from the correlated NRTL parameters. All ternary systems were classified as Treybal's type II, which have two immiscible binaries [29]. Hexane was almost immiscible with all kinds of ILs used in this work, all of which have a hydrophobic anion. As illustrated in Table 4, the solubility of benzene is higher in [BMIM][PF_6] than in other ILs in broader concentration ranges. Therefore, we've used [BMIM][PF_6] as a solvent for other aromatics: toluene and p-xylene.

The distribution coefficient (D) and selectivity (S) of the ionic liquids in Table 4 were determined from the equation below:

$$D = \frac{w_2^i}{w_2^h} \tag{5}$$

$$S = \frac{w_2^i \cdot w_1^h}{\chi_1^i \cdot \chi_2^h} \tag{6}$$

Table 4. Experimental mass fraction (w) of tie-lines, distribution coefficient (D) and selectivity (S) at T=298.15 K

Hexane-rich phase		ILs-rich phase		D	S
w_1^h	w_2^h	w_1^i	w_2^i		
{Hexane (1)+benzene (2)+[BMIM][Tf_2N] (3)}					
0.9958	0.0000	0.0136	0.0000	-	-
0.9341	0.0638	0.0200	0.0290	0.4545	21.2296
0.8539	0.1442	0.0216	0.0645	0.4473	17.6827
0.6571	0.3395	0.0275	0.1490	0.4389	10.4869
0.4948	0.5035	0.0299	0.2143	0.4256	7.0434
0.3436	0.6542	0.0296	0.2752	0.4207	4.8831
0.2467	0.7479	0.0280	0.3168	0.4236	3.7321
0.1494	0.8409	0.0141	0.3666	0.4360	4.6193
{Hexane (1)+benzene (2)+[BMIM][PF_6] (3)}					
0.9988	0.0000	0.0075	0.0000	-	-
0.7646	0.2327	0.0085	0.0751	0.3227	29.0308
0.5749	0.4207	0.0087	0.1355	0.3221	21.2833
0.4980	0.5010	0.0081	0.1629	0.3252	19.9907
0.4125	0.5846	0.0079	0.1903	0.3255	16.9972
0.3695	0.6238	0.0076	0.2093	0.3355	16.3127
0.2364	0.7610	0.0065	0.2558	0.3361	12.2250
0.2893	0.7089	0.0074	0.2369	0.3342	13.0646
{Hexane (1)+benzene (2)+[EMIM][Tf_2N] (3)}					
0.9972	0.0000	0.0045	0.0000	-	-
0.8990	0.1000	0.0096	0.0343	0.3430	32.1205
0.8008	0.1980	0.0104	0.0659	0.3328	25.6278
0.7104	0.2885	0.0145	0.1075	0.3726	18.2557
0.6286	0.3683	0.0138	0.1320	0.3574	16.3255
0.6040	0.3943	0.0128	0.1441	0.6545	17.2450
0.5751	0.4215	0.0147	0.1596	0.3786	14.8136
0.5232	0.4744	0.0141	0.1762	0.3714	13.7819
0.4587	0.5377	0.0159	0.1999	0.3718	10.7252
0.3527	0.6443	0.0160	0.2339	0.3630	8.0025
0.1936	0.7993	0.0138	0.3020	0.3778	5.3006
0.1102	0.8884	0.0115	0.3381	0.3806	3.6800
{Hexane (1)+benzene (2)+[OMIM][BF_4] (3)}					
0.9945	0.0000	0.0420	0.0000	-	-
0.7772	0.2203	0.0600	0.1079	0.4898	6.3444
0.5990	0.3993	0.0610	0.2006	0.5024	4.9332
0.5281	0.4705	0.0639	0.2347	0.4988	4.1226
0.4423	0.5503	0.0631	0.2806	0.5099	3.5742
0.3790	0.6090	0.0610	0.3105	0.5099	3.1678
0.2619	0.7263	0.0453	0.3743	0.5154	2.9795
0.1547	0.8291	0.0293	0.4405	0.5313	2.8052

Table 4. Continued

Hexane-rich phase		ILs-rich phase		D	S
w_1^h	w_2^h	w_1^i	w_2^i		
{Hexane (1)+toluene (2)+[BMIM][PF_6] (3)}					
0.9951	0.0000	0.0038	0.0000	-	-
0.7162	0.2830	0.0053	0.0256	0.0905	12.2240
0.4751	0.5235	0.0059	0.0870	0.1662	13.3372
0.3672	0.6325	0.0051	0.1298	0.2052	14.7757
0.2180	0.7805	0.0048	0.1832	0.2347	10.5941
0.1632	0.8313	0.0047	0.2100	0.2526	8.7717
0.1096	0.8886	0.0032	0.2352	0.2647	9.0655
0.0880	0.9103	0.0039	0.2685	0.2950	6.6555
{Hexane (1)+p-xylene (2)+[BMIM][PF_6] (3)}					
0.9988	0.0000	0.0068	0.0000	-	-
0.7797	0.2200	0.0070	0.0272	0.1236	13.7893
0.5994	0.4002	0.0055	0.0480	0.1199	13.1654
0.4446	0.5545	0.0054	0.0592	0.1068	8.7679
0.3515	0.6468	0.0036	0.0729	0.1127	11.0468
0.2232	0.7752	0.0034	0.0892	0.1151	7.6279
0.1837	0.8149	0.0029	0.0946	0.1161	7.3432

Combined standard uncertainty u_c is $u_c(w)=3\times10^{-4}$ and standard uncertainty u is u(T)=0.02 K

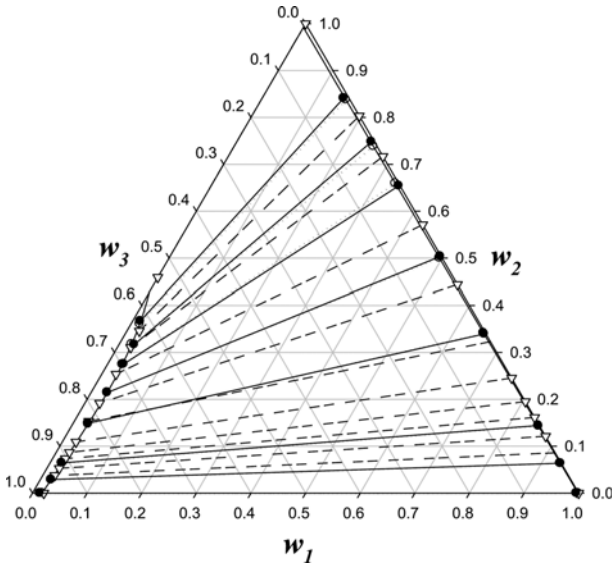

Fig. 2. Tie lines for the ternary mixture of {hexane (1)+benzene (2)+[BMIM][Tf_2N] (3)} at 298.15 K; ●, experimental value; ○, calculated values by NRTL model; ●-●, experimental tie line; ○··○, tie line from NRTL model; ▽- -▽, experimental tie line from Ref. [10].

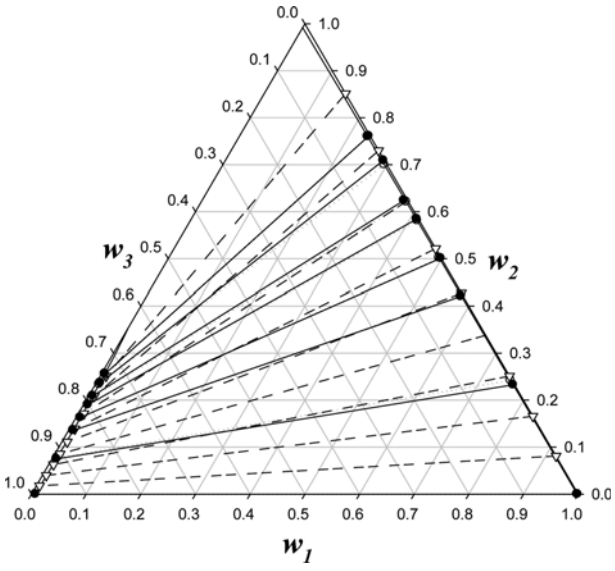

Fig. 3. Tie lines for ternary mixture of {hexane (1)+benzene (2)+ [BMIM][PF_6] (3)} at 298.15 K; ●, experimental value; ○, calculated values by NRTL model; ●-●, experimental tie line; ○··○, tie line from NRTL model; ▽- -▽, experimental tie line from Ref. [11].

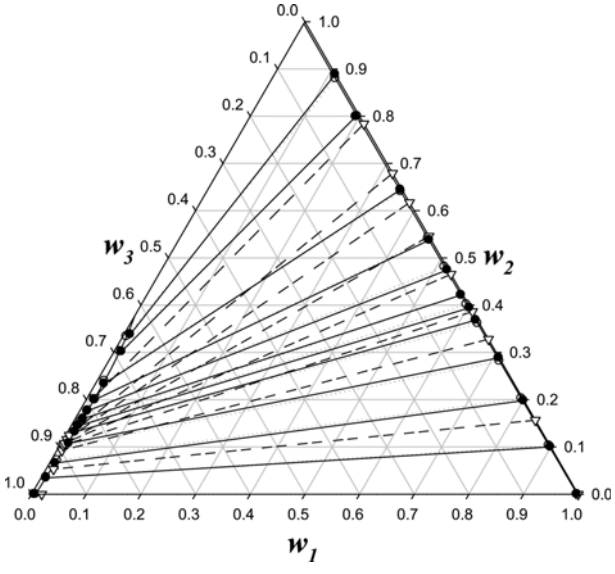

Fig. 4. Tie lines for ternary mixture of {hexane (1)+benzene (2)+ [EMIM][Tf_2N] (3)} at 298.15 K; ●, experimental value; ○, calculated values by NRTL model; ●-●, experimental tie line; ○··○, tie line from NRTL model; ▽- -▽, experimental tie line from Ref. [12].

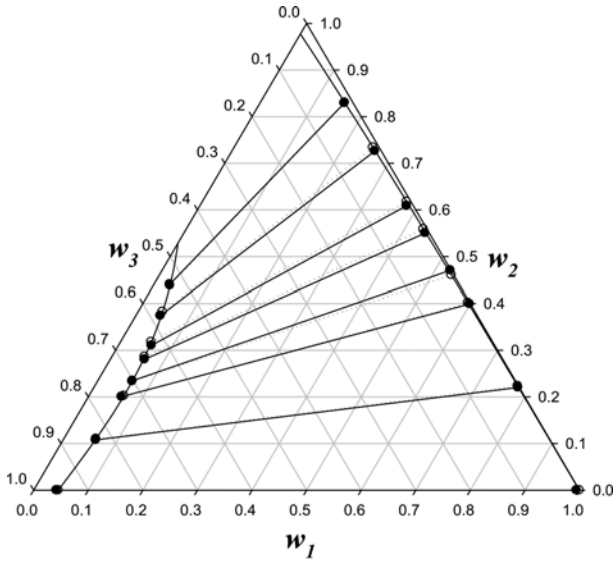

Fig. 5. Tie lines for ternary mixture of {hexane (1)+benzene (2)+ [OMIM][BF_4] (3)} at 298.15 K; ●, experimental value; ○, calculated values by NRTL model; ●-●, experimental tie line; ○··○, tie line from NRTL model.

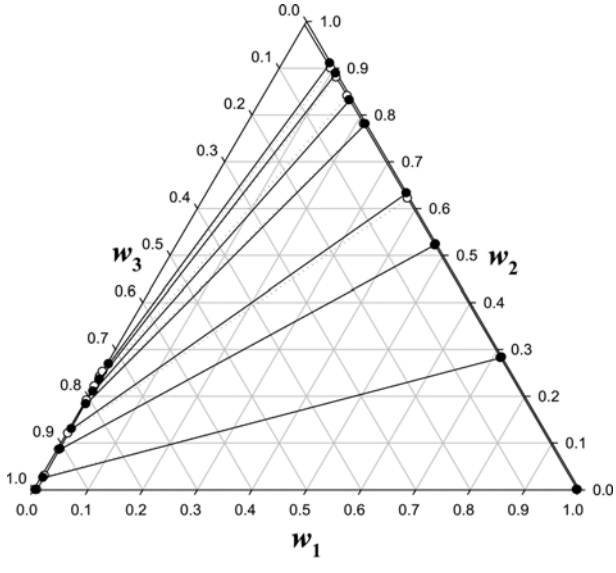

Fig. 6. Tie lines for ternary mixture of {hexane (1)+toluene (2)+ [BMIM][PF_6] (3)} at 298.15 K; ●, experimental value; ○, calculated values by NRTL model; ●-●, experimental tie line; ○··○, tie line from NRTL model.

where w_1 and w_2 refer to mass fractions of the hexane and benzene, and x_1 and x_2 are the mole concentration of hexane and benzene, respectively. The superscripts, i and h, refer to the ionic liquid-rich (extract) phase and to the hexane-rich (raffinate) phase, respectively. Here, the D and S values were calculated by using the mass fractions instead of the mole fractions because the ILs have a much higher molecular weight than the studied alkanes [8]. The D values according to the concentration of BTX aromatics in different ternary systems are illustrated in Fig. 8. As shown in the figure, the D values obtained in this work are less than unity and did not vary significantly with the amount of benzene. The organic solvents, acetonitrile and sulfolane, that were selected for comparison, show slightly larger D values than the ILs, and acetonitrile shows the largest D values among the considered solvent systems. By contrast, as shown in Fig. 9, all the S values of the IL solvents are much higher than unity and much greater than that of the organic solvent, acetonitrile. In the meanwhile, the value of S obtained for sulfolane approximated the median of the values determined for the ILs in

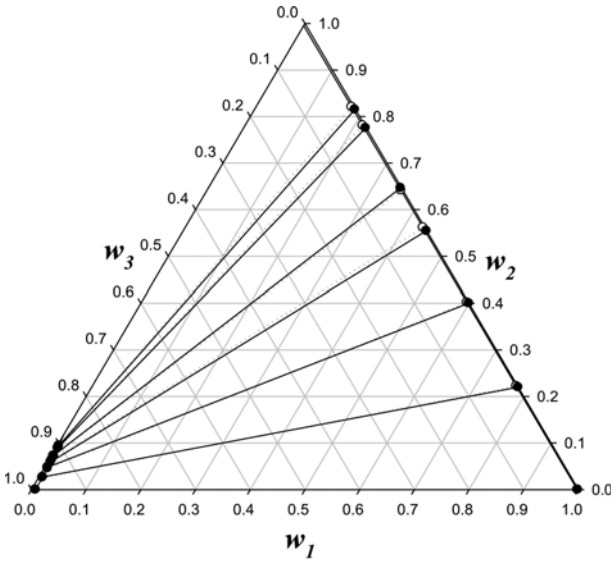

Fig. 7. Tie lines for ternary mixture of {hexane (1)+p-xylene (2)+[BMIM][PF_6] (3)} at 298.15 K; ●, experimental value; ○, calculated values by NRTL model; ●-●, experimental tie line; ○··○, tie line from NRTL model.

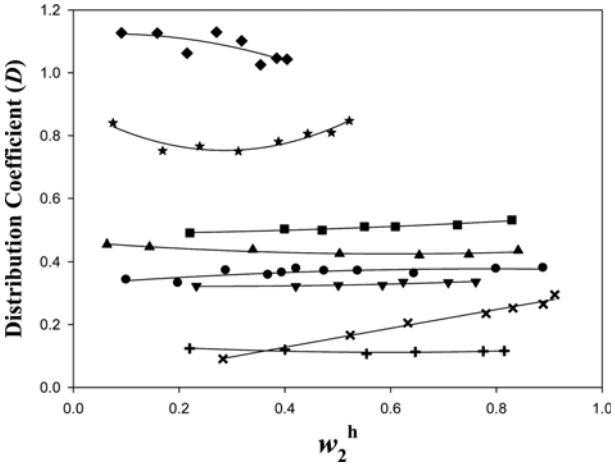

Fig. 8. Distribution coefficient (D) versus w_2^h for the ternary systems at 298.15 K; ▲, {hexane (1)+benzene (2)+[BMIM][Tf_2N] (3)}; ▼, {hexane (1)+benzene (2)+[BMIM][PF_6] (3)}; ●, {hexane (1)+benzene (2)+[EMIM][Tf_2N] (3)}; ■, {hexane (1)+benzene (2)+[OMIM][BF_4] (3)}; ×, {hexane (1)+toluene (2)+[BMIM][PF_6] (3)}; +, {hexane (1)+p-xylene (2)+[BMIM][PF_6] (3)}; ◆, {hexane (1)+benzene (2)+acetonitrile (3)}; from Ref. [15]; ★, {hexane (1)+toluene (2)+sulfolane (3)}; from Ref. [27].

this work. The selectivity of benzene in the IL-rich phase increased with decreasing aromatic concentration in the raffinate phase. In Fig. 9, the selectivity data, of which those of sulfolane and acetonitrile were obtained from the literature, were used to enable a more accurate comparison [15,30]. As shown in Fig. 9, among the solvents studied in this work, [BMIM][PF_6] had the largest S values, followed by [EMIM][Tf_2N] in broader concentration ranges.

The *S* values of benzene contained systems decreased in the

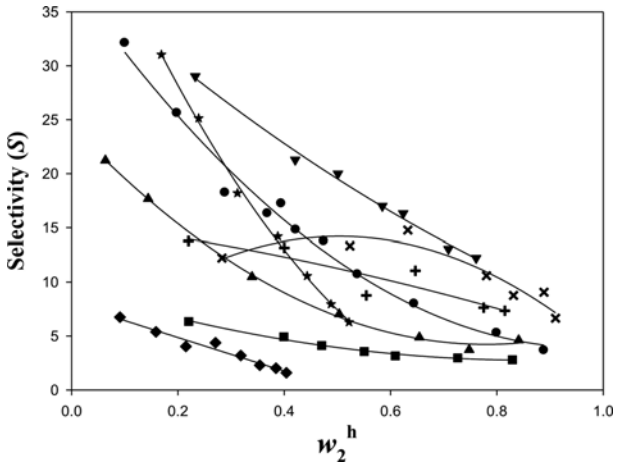

Fig. 9. Selectivity (S) versus w_2^h for the ternary systems at 298.15 K; ▲, {hexane (1)+benzene (2)+[BMIM][Tf_2N] (3)}; ▼, {hexane (1)+benzene (2)+[BMIM][PF_6] (3)}; ●, {hexane (1)+benzene (2)+[EMIM][Tf_2N] (3)}; ■, {hexane (1)+benzene (2)+[OMIM][BF_4] (3)}; ×, {hexane (1)+toluene (2)+[BMIM][PF_6] (3)}; +, {hexane (1)+p-xylene (2)+[BMIM] [PF_6] (3)}; ◆, {hexane (1)+benzene (2)+acetonitrile (3)}; from Ref. [15]; ★, {hexane (1)+toluene (2)+sulfolane (3)}; from Ref. [27].

order of [BMIM][PF_6]>[EMIM][Tf_2N]>sulfolane>[BMIM] [Tf_2N]>[OMIM][BF_4]>acetonitrile. Therefore, the considered imidazolium-based ILs examined in this work have been shown to be effective for use as selective solvents in the benzene recovery process. Furthermore, these ILs can be used to replace toxic organic solvents with a high selectivity for aromatic compounds in mixtures consisting of aliphatic and aromatic components, especially in mixtures with low concentrations of aromatic compounds.

3. Thermodynamic Correlation and Reliability of the Experimental LLE Data

The experimental binary and ternary LLE data were correlated with the NRTL equation [31]. The NRTL equations for the activity coefficient in multicomponent systems are:

$$\ln\gamma_i = \frac{\Sigma_j \tau_{ji} G_{ji} x_j}{\Sigma_k G_{ki} x_k} + \sum_j \frac{x_j G_{ij}}{\Sigma_k G_{kj} x_k}\left[\tau_{ij} - \frac{\Sigma_k x_k \tau_{kj} G_{ki}}{\Sigma_k G_{kj} x_k}\right] \quad (7)$$

$$\tau_{ij} = \frac{\Delta g_{ij}}{RT} \quad (\tau_{ij} \neq \tau_{ji}) \quad (8)$$

$$G_{ij} = \exp(-\alpha_{ij}\tau_{ij}) \quad (\alpha_{ij} = \alpha_{ji}) \quad (9)$$

The adjustable parameters for each binary pair τ_{ij}, τ_{ji} are related to the characteristic energy of interaction between the molecules of type i and j, and α_{ij} is related to the non-randomness of the mixture [32]. The non-randomness parameter (α_{ij}) was set to 0.20 in this work to avoid an erroneous liquid-liquid description. Moreover, the sub-binary model parameters (g_{ij}) were calculated individually from the experimental LLE data for each of the systems, since it provides a better correlation result for the LLE data reduction [7,33].

The objective function (OF) that was used served to minimize the differences between the experimental and calculated mass fraction of the components in both phases.

Table 5. The NRTL model parameters and the calculated RMSD

System	NRTL parameters (α_{ij}=0.20)			RMSD
	i-j	$(g_{ij}-g_{ii})/R$ (K)	$(g_{ji}-g_{jj})/R$ (K)	
{Hexane (1)+benzene (2)+[BMIM][Tf_2N] (3)}	1-2	396.96	−315.93	0.0033
	2-3	1693.30	−270.78	
	1-3	1559.20	699.44	
{Hexane (1)+benzene (2)+[BMIM][PF_6] (3)}	1-2	−181.73	229.98	0.0031
	2-3	1592.50	−179.06	
	1-3	1381.80	947.00	
{Hexane (1)+benzene (2)+[EMIM][Tf_2N] (3)}	1-2	233.68	−225.74	0.0040
	2-3	1833.30	−227.72	
	1-3	1399.30	944.61	
{Hexane (1)+benzene (2)+[OMIM][BF_4] (3)}	1-2	542.40	−450.50	0.0042
	2-3	1502.60	−329.37	
	1-3	2019.10	470.04	
{Hexane (1)+toluene (2)+[BMIM][PF_6] (3)}	1-2	−458.57	49.94	0.0064
	2-3	1576.00	−111.58	
	1-3	1200.30	984.74	
{Hexane (1)+p-xylene (2)+[BMIM][PF_6] (3)}	1-2	−138.12	138.03	0.0036
	2-3	1500.60	214.49	
	1-3	1482.90	899.84	

Table 6. Othmer-Tobias parameters and the linear correlation parameter (R^2)

System	A	B	R^2
{Hexane (1)+benzene (2)+[BMIM][Tf_2N] (3)}	1.7667	2.2672	0.9900
{Hexane (1)+benzene (2)+[BMIM][PF_6] (3)}	2.0153	3.2460	0.9955
{Hexane (1)+benzene (2)+[EMIM][Tf_2N] (3)}	1.5494	2.3754	0.9810
{Hexane (1)+benzene (2)+[OMIM][BF_4] (3)}	2.1929	1.8204	0.9901
{Hexane (1)+toluene (2)+[BMIM][PF_6] (3)}	1.5824	3.7901	0.9813
{Hexane (1)+p-xylene (2)+[BMIM][PF_6] (3)}	2.9337	8.0565	0.9938

$$OF = \min \sum_i \sum_\alpha \sum_k \left(w_{ik}^{\alpha(exp)} - w_{ik}^{\alpha(cal)}\right)^2 \quad (10)$$

The calculated equilibrium compositions, $w_{ik}^{\alpha(cal)}$ were compared with the experimental tie-line data, $w_{ik}^{\alpha(exp)}$ and the subscripts i, α, and k denote the component, phase, and tie line, respectively. The root mean square deviation (RMSD) was calculated to evaluate the agreement between the experimental data and the calculated results according to the following equation:

$$RMSD = \sqrt{\frac{\sum_i \sum_\alpha \sum_k \left(w_{ik}^{\alpha(exp)} - w_{ik}^{\alpha(cal)}\right)^2}{6N}} \quad (11)$$

where N is the number of tie-lines. The solid lines in Figs. 2-7 represent the values calculated using the NRTL model. All the correlation parameters and the RMSD, determined by the NRTL model, are given in Table 5. The RMSD provides a measure of the accuracy of the correlations. All of the RMSD values in Table 5 are below 0.0064 at 298.15 K, indicating that the LLE experimental data correlated well with the data that was obtained by using the NRTL model.

The reliability of the determined LLE data was validated by using the Othmer-Tobias correlation [13]:

$$\ln\left(\frac{1-w_1^h}{w_1^h}\right) = A\ln\left(\frac{1-w_3^i}{w_3^i}\right) + B \quad (12)$$

where w_1 and ws_3 refer to the mass fractions of the hexane and ILs, respectively, and *A*, the *angular coefficient* and *B*, the *linear coefficient* are the adjustable parameters of the Othmer-Tobias equation. The superscripts h and i refer to the hexane-rich and IL-rich phases, respectively. The linearity of these fittings indicates the degree of consistency of the experimental LLE data. Table 6 lists the values of parameters A and B together with the linear correlation coefficient, R^2. The linearity of the Othmer-Tobias plot indicates the high degree of consistency of the experimental data. The R^2 values of the fittings are very close to 1, which indicates a good degree of consistency for all the determined ternary LLE data.

CONCLUSIONS

LLE data were determined for a binary system {hexane (1)+[BMIM][Tf_2N] (2)} and six ternary systems: {hexane (1)+benzene (2)+[BMIM][Tf_2N] (3)}, {hexane (1)+benzene (2)+[BMIM][PF_6] (3)}, {hexane (1)+benzene (2)+[EMIM][Tf_2N] (3)}, {hexane (1)+benzene (2)+[OMIM][BF_4] (3)}, {hexane (1)+toluene (2)+[BMIM]

$[PF_6]$ (3)}, {hexane (1)+p-xylene (2)+[BMIM][PF_6] (3)} at 298.15 K and atmospheric pressure. The ternary systems were classified as Treybal's type II. The binary and ternary data correlated well with NRTL model with RMSD values less than 0.0064. According to the binary LLE data for {hexane (1)+[BMIM][Tf_2N] (2)}, hexane was more soluble in [BMIM][Tf_2N] than vice versa. The results of the Othmer-Tobias test showed the determined ternary LLE data to have a good consistency. The calculated distribution coefficient (D) and selectivity (S) values of the ILs as solvents show slightly smaller values of D and much higher values of S compared to those of conventional organic solvents, acetonitrile, and sulfolane. [BMIM][PF_6] showed largest S to benzene, followed by [EMIM][Tf_2N] in broader solute concentration ranges. The results of this work indicate that the imidazolium-based ILs can be used as selective non-toxic solvents in the BTX aromatics recovery process, and that they could be a good substitute for toxic organic solvents in aromatic-aliphatic mixture separations.

ACKNOWLEDGEMENTS

This work was supported by research fund of Chungnam National University, Daejeon, Republic of Korea.

REFERENCES

1. K. Weissermel and H.-J. Arpe, *Industrial Organic Chemistry*, 4th Ed., Wiley-VCH: Weinheim, Germany (2003).
2. G. W. Meindersma, J. G. Podt and A. B. de Haan, *J. Chem. Eng. Data*, **51**, 1814 (2006).
3. M. J. Earl and K. R. Seddon, *Pure Appl. Chem.*, **72**, 1391 (2000).
4. C. P. Gredlake, J. M. Crosthwaite, D. G. Hert, S. N. Aki and J. F. Brennecke, *J. Chem. Eng. Data*, **49**, 954 (2004).
5. G. W. Meindersma, J. G. Podt and A. B. de Haan, *Fluid Phase Equilib.*, **247**, 158 (2006).
6. C. B. Manohar, D. Rabari, A. A. Kumar and T. Banerjee, *Fluid Phase Equilib.*, **360**, 392 (2013).
7. R. M. Maduro and M. Aznar, *Fluid Phase Equilib.*, **265**, 129 (2008).
8. S. Corderí, E. J. González, N. Calvar and A. Domínguez, *J. Chem. Thermodynamics*, **53**, 60 (2012).
9. G. W. Meindersma, A. R. Hansmeir and A. B. de Haan, *Ind. Eng. Chem. Res.*, **49**, 7530 (2010).
10. N. Calvar, I. Domínguez, E. Gómez and A. Domínguez, *Chem. Eng. J.*, **175**, 213 (2011).
11. O. A. Al-Rashed, M. A. Fahim and M. Shaaban, *Fluid Phase Equilib.*, **363**, 248 (2014).
12. A. Arce, M. J. Earle, H. Rodríquez and K. R. Seddon, *J. Phys. Chem. B*, **111**, 4732 (2007).
13. D. F. Othmer and P. E. Tobias, *Ind. Eng. Chem.*, **34**, 693 (1942).
14. T. J. Afolabi and A. I. Alao, *Fluid Phase Equilib.*, **379**, 19 (2014).
15. S. Yang, Y. Wang, X. Qi and J. Wang, *Fluid Phase Equilib.*, **367**, 69 (2014).
16. S. Viswanathan, M. Anand Rao and D. H. Prasad, *J. Chem. Eng. Data*, **45**, 764 (2000).
17. M. I. Aralaguppi, C. V. Jadar and T. M. Aminabhavi, *J. Chem. Eng. Data*, **44**, 446 (1999).
18. U. Domanska, *Fluid Phase Equilib.*, **130**, 207 (1997).
19. C. Diaz, A. Dominguez and J. Tojo, *J. Chem. Eng. Data*, **47**, 867 (2002).
20. Dortmund Data Bank Software Package (DDBSP), Version 2013 professional.
21. S. Zhao, P. Bai and C. Sun, *Fluid Phase Equilib.*, **375**, 37 (2014).
22. G. Singh and A. Kumar, *Indian J. Chem.*, **47**, 495 (2008).
23. A. Arce, E. Rodil and A. Soto, *J. Solution Chem.*, **35**, 63 (2006).
24. A. Laesecke and T. J. Fortin, *Energy Fuels*, **26**, 1844 (2012).
25. T. J. Fortin, A. Laesecke, M. Freund and S. Outcalt, *J. Chem. Thermodyn.*, **57**, 276 (2013).
26. R. D. Chirico, M. Frenkel, J. W. Magee, V. Diky, C. D. Muzny, A. F. Kazakov, K. Kroenlein, I. Abdulagatov, G. R. Hardin, W. E. Acree, J. F. Brenneke, P. L. Brown, P. T. Cummings, T. W. de Loos, D. G. Friend, A. R. H. Goodwin, L. D. Hansen, W. M. Haynes, N. Koga, A. Mandelis, K. N. Marsh, P. M. Mathias, C. McCabe, J. P. O'Connell, A. Padua, V. Rives, C. Schick, J. P. M. Trusler, S. Vyazovkin, R. D. Weir and J. Wu, *J. Chem. Eng. Data*, **58**, 2699 (2013).
27. I. Y. Jeong, S. H. You and S. J. Park, *Fluid Phase Equilib.*, **378**, 93 (2014).
28. I. C. Hwang and S. J. Park, *Fluid Phase Equilib.*, **301**, 18 (2011).
29. R. E. Treybal, *Liquid Extraction*, 2nd Ed., McGraw-Hill press: New York (1963).
30. M. Mukhopadhyay and K. R. Dongaonkar, *Ind. Eng. Chem. Process Des. Dev.*, **22**, 521 (1983).
31. H. Renon and J. M. Prausnitz, *AIChE J.*, **14**, 135 (1968).
32. S. H. You, I. Y. Jeong and S. J. Park, *Fluid Phase Equilib.*, **389**, 9 (2015).
33. E. J. González, N. Calvar, E. Gómez and A. Domínguez, *Fluid Phase Equilib.*, **303**, 174 (2011).